



How close to two dimensions does a Lennard-Jones system need to be to produce a hexatic phase?

Nadezhda Gribova, Axel Arnold, Tanja Schilling, and Christian Holm

Citation: *J. Chem. Phys.* **135**, 054514 (2011); doi: 10.1063/1.3623783

View online: <http://dx.doi.org/10.1063/1.3623783>

View Table of Contents: <http://jcp.aip.org/resource/1/JCPSA6/v135/i5>

Published by the [AIP Publishing LLC](http://www.aip.org).

Additional information on J. Chem. Phys.

Journal Homepage: <http://jcp.aip.org/>

Journal Information: http://jcp.aip.org/about/about_the_journal

Top downloads: http://jcp.aip.org/features/most_downloaded

Information for Authors: <http://jcp.aip.org/authors>

ADVERTISEMENT

The advertisement features the NVIDIA logo on the left, which includes a green square with a stylized eye and the word 'NVIDIA' in white. To the right of the logo, the text 'RUN YOUR GPU CODE 2X FASTER.' is written in white, followed by 'TRY A TESLA K20 GPU ACCELERATOR TODAY. FREE.' in green. The background of the advertisement is a dark, abstract image with colorful, glowing lines and patterns, suggesting a high-tech or scientific environment.

**RUN YOUR GPU
CODE 2X FASTER.
TRY A TESLA K20 GPU
ACCELERATOR TODAY.
FREE.**

How close to two dimensions does a Lennard-Jones system need to be to produce a hexatic phase?

Nadezhda Gribova,^{1,2,a)} Axel Arnold,^{1,b)} Tanja Schilling,³ and Christian Holm¹

¹*Institute for Computational Physics, University of Stuttgart, Pfaffenwaldring 27, D-70569 Stuttgart, Germany*

²*Institute for High Pressure Physics, Russian Academy of Sciences, Troitsk 142190, Moscow Region, Russia*

³*Université du Luxembourg, 162 A, Avenue de la Faïencerie L-1511 Luxembourg*

(Received 4 April 2011; accepted 19 July 2011; published online 5 August 2011)

We report on a computer simulation study of a Lennard-Jones liquid confined in a narrow slit pore with tunable attractive walls. In order to investigate how freezing in this system occurs, we perform an analysis using different order parameters. Although some of the parameters indicate that the system goes through a hexatic phase, other parameters do not. This shows that to be certain whether a system of a finite particle number has a hexatic phase, one needs to study not only a large system, but also several order parameters to check all necessary properties. We find that the Binder cumulant is the most reliable one to prove the existence of a hexatic phase. We observe an intermediate hexatic phase only in a monolayer of particles confined such that the fluctuations in the positions perpendicular to the walls are less than 0.15 particle diameters, i.e., if the system is practically perfectly 2D.

© 2011 American Institute of Physics. [doi:10.1063/1.3623783]

I. INTRODUCTION

Understanding the structure and dynamics of confined fluids is important for processes, such as wetting, coating, and nucleation. The properties of a fluid confined in a pore differ significantly from the bulk fluid due to finite size effects, surface forces, and reduced dimensionality. In this work, we report on a study of one of the simplest models that is still capable of reproducing the thermodynamic behavior of classical fluids, the Lennard-Jones (LJ) system. The LJ potential is an important model for exploring the behavior of simple fluids and has been used to study homogeneous vapor-liquid, liquid-liquid, and liquid-solid equilibrium, melting, and freezing.^{1–3} It has also been used as a reference fluid for complex systems such as colloidal and polymeric systems.

The vapor-to-liquid transition in confined systems has been studied intensively and is well understood (see Ref. 4 and references therein). In this article, we will discuss the liquid-to-solid transition in a slit pore and the process of the development of the solid phase. In the liquid phase, confinement to a slit induces layering at the walls. One could imagine this effect to facilitate crystallization. And indeed it is known that depending on the strength of the particle-wall interaction, the freezing scenario changes significantly.^{1,5} If the walls are strongly attractive, crystallization starts from the walls and at a temperature higher than without confinement. If the walls are strongly repulsive, crystallization starts from the bulk at a temperature lower than without confinement.

A well-distinguished layer of particles close to the wall can also, to some extent, be treated as a 2D system. The melting of true 2D systems has been studied both theoretically^{6–10}

and experimentally.^{11–13} A large number of experiments on 2D melting were carried out in colloidal systems where colloidal particles contain a magnetic core, giving rise to a magnetic repulsion between particles that can be controlled by an external magnetic field (see, for example, Refs. 14–16). The type of the scenario strongly depends on the shape of the potential. Soft-core potentials melt via the Kosterlitz-Thouless-Halperin-Nelson-Young (KTHNY) mechanism,^{7,9} meaning that the liquid turns into a crystal going through an intermediate hexatic phase.^{17–21} For the hard disks system, two different points of view exist.^{7,8,10,22} Since the Lennard-Jones potential is rather soft, the freezing of a single layer of LJ particles can, therefore, be expected to proceed via the KTHNY mechanism,²³ which significantly differs from the bulk nucleation scenario.

As we will show, it can be difficult to check whether the hexatic phase exists if one studies a system of a finite particle number. To solve this problem, several order parameters to characterize the bond-order were introduced in the literature. The correlation function of the local bond-order parameter²¹ that measures the nearest-neighbor-bond-angular order is commonly used. However, it cannot distinguish between a hexatic phase and a heterogeneous system in the two-phase region. The distribution of the bond-angular susceptibility on various length scales was introduced to overcome this problem studying a hard disk system and Lennard-Jones disks.²⁴ Later the search for a general and efficient method to determine all phases and bounds of the transition was continued. The scale analysis of the behavior of the fluctuations of the bond-angular susceptibility and the bond-orientation cumulant provided²⁵ an evidence of a possible continuous transition in the system of hard disks.¹⁰ To our knowledge, the Binder cumulant was applied in the analysis of the existence of the hexatic phase only for 2D systems and never for quasi-2D or 3D. The analysis of fluctuations of the bond-angular susceptibility within a layer was used already for studying

^{a)}Present address: Institute of Thermodynamics and Thermal Process Engineering, University of Stuttgart, Pfaffenwaldring 9, D-70569 Stuttgart, Germany; Electronic mail: gribova@icp.uni-stuttgart.de.

^{b)}Previous address: Fraunhofer SCAI, Schloss Birlinghoven, D-53754 Sankt Augustin, Germany.

the melting of thin films up to 20 layers.²⁶ A modified scaling analysis of the bond-angular susceptibility²⁷ was used not to check the existence of the hexatic phase only in 2D systems,^{8,27,28} but also in quasi-2D systems, for example, see Ref. 29.

Another method used in 2D systems to check if the transition is of KTHNY type is to study the elastic properties of the system.^{30–32} If Young's modulus in the solid is less than $16\pi k_B T$, then it is very likely that the solid melts via dislocation unbinding. On the other hand, if this value is reached already in the liquid, the transition is likely to be of first order. However, based only on the elastic properties one cannot distinguish a two-phase region from a hexatic phase. There is also some discrepancy in results depending on the method by which the elastic constants were obtained.³²

In the thermodynamic limit, all above-mentioned parameters allow to safely distinguish a homogeneous solid, liquid, or hexatic phase. However, both in simulations as well as in many experiments, one never reaches the thermodynamic limit. Moreover, experiments especially on colloids are in fact often performed in the NVT ensemble, in which case also phase coexistence can easily appear. The latter can be excluded by finite size scaling, but even then, due to their different functional dependences on the system size, not all parameters are equally well suited to determine the phase behavior of a given system.

The question, how the crystallization in a strongly confined quasi-2D system proceeds, i.e., in a system only a couple of particle diameters wide, is less well studied than the crystallization in a pure 2D system. In this case, it is not clear whether the system still behaves like being truly two dimensional, or whether it rather behaves similar to a bulk system. This question is certainly even more difficult to tackle than nucleation in a purely 2D or 3D system and has been mostly addressed by means of computer simulations so far. Under these circumstances, it is particularly important to have reliable order parameters to detect or exclude the existence of a hexatic phase from computer simulations.

The solid-solid phase transitions of confined fluids in narrow slit pores were studied both at zero and at finite temperatures (see Refs. 33–35 and references therein). For a confined LJ fluid, the question if a hexatic phase exists in a quasi-2D system has been studied by Radhakrishnan and co-workers³⁶ for a ratio of wall-particle to particle-particle attraction varying between 0 and 2.14 and pores widths of 3 and 7.5 fluid particle diameters. For the narrower slit pore, it was shown that around the freezing temperature the system exhibits a hexatic phase. With increasing wall attraction this temperature region becomes wider, i.e., an attractive wall facilitates the formation of the hexatic phase. The phase diagram for the wider pore with diameter 7.5 is more complicated. When the wall-particle attraction becomes bigger than the particle-particle attraction, at first a hexatic phase and then a crystal phase appear, however, only in the contact layers near the walls; the rest of the system remains liquid. Only when decreasing the temperature further, the system crystallizes completely. The temperature range, in which a hexatic or a hexatic phase is observed only in the contact layers, again widens with growing wall-particle attraction. This indicates that the

wall-particle attraction facilitates the formation of a hexatic phase even in wider pores, however, only in the layers close to the walls. The same group of authors also reported that in a pore, that can accommodate only a single layer, two second order transitions are observed, while already in a pore wide enough to accommodate two layers, both transitions are of the first order.²⁹

The different crystal structures of the frozen phase were studied by Vishnyakov and Neimark³⁷ as a function of the size of the slit for this system. The distance between the walls was gradually increased up to a slit accommodating three layers. Depending on the width of the pore, a hexagonal or orthorhombic phase was observed in the layers.

In a recent article by Page and Sear,³⁸ it was shown that freezing is controlled by prefreezing in a similar system. Nucleation of the bulk crystal is affected by the surface phase behavior. With increasing wall attraction, the bulk nucleation is smoothly transformed into nucleation of a surface crystal layer. Xu and Rice³⁹ investigated theoretically a quasi-2D system of hard spheres and reported the dependence of the density at the liquid-to-hexatic phase transition on the thickness of the system, with wall separation changing from 1 to 1.6 hard sphere diameters. For the current state of art in crystallization of confined systems, we recommend to consult recent reviews.^{2,3,22}

In this paper, we investigate a Lennard-Jones fluid confined between two planar walls at different values of wall-particle attraction during freezing and melting. The walls form an attractive slit pore with changing wall separation, that is able to accommodate 1 or 2 layers. To characterize and distinguish the liquid, hexatic and solid phases, we investigate several order parameters and compare their behavior. We show that those parameters are not equally reliable when it comes to predicting the existence of a hexatic phase from finite size configurations.

By combining several of the parameters, we can drastically narrow down the possible range of a hexatic phase. Most notably, we cannot find such a phase in multilayer systems, as predicted by Radhakrishnan *et al.*^{29,36} With just two layers, we always observe phase coexistence of solid and liquid, rather than a hexatic phase. Even in a single layer, we find a possible hexatic phase only for very strong confinement, which can explain some controversy in experiments regarding the observation of a hexatic phase.^{40,41}

The article is structured as follows. In Sec. II, we describe our simulation method, and in Sec. III we present the order parameters and the results. We conclude with a summary in Sec. IV.

II. SIMULATION METHOD

We performed molecular dynamics (MD) simulations of Lennard-Jones particles confined between two structureless walls. The particles interact via the LJ-potential

$$u(r) = 4\epsilon \left[\left(\frac{\sigma}{r} \right)^{12} - \left(\frac{\sigma}{r} \right)^6 \right], \quad (1)$$

where r is the distance between the particles, σ is the particle diameter, and ϵ is the depth of the minimum of the LJ

potential. The interaction between walls and particles is given by a LJ-potential integrated over semi-space,

$$u_w(r) = 4\epsilon_w \left[\left(\frac{\sigma}{r} \right)^9 - \left(\frac{\sigma}{r} \right)^3 \right]. \quad (2)$$

The particle-particle interaction was cutoff and shifted at a distance $r_c = 2.5\sigma$ and the wall-particle interaction at a distance $r_c = 4.0\sigma$, since the wall-particle potential is wider and deeper than the particle-particle potential. For the following, we will use ϵ as the unit of energy, σ as the unit of length, and $\tau = \sqrt{1 \cdot \sigma^2 / \epsilon}$ as unit of time (i.e., use the particle mass as the unit of mass); consequently, temperatures are given in multiples of $\epsilon/k_B T$. The simulations were performed in a cuboid box with periodic boundary conditions in the x and y directions and two walls positioned at $z = 0$ and L_z . The distance between the walls was chosen such that $n = 1$ or 2 layers can be accommodated in the pore, namely $L_z = 2 \times 1.12 + 0.916(n - 1)$. Here, 1.12 is the distance at which the wall potential has its minimum, and 0.916 is the layer distance in an ideal FCC lattice with spacing one. Therefore, L_z was either 2.24 or 3.16 for one or two layers, respectively, while the other two dimensions of the simulation box were fixed as $L_x = L_y = 200$, if not otherwise stated. The number of particles N was chosen such that the density was kept constant at one particle per unit cube independent of the width of the slit, and therefore ranged from 44 800 for one layer to 81 600 particles for two layers. Since the slit is narrow, layering in the two layered system is observed in the whole range of the temperatures.

We carried out our simulations out in the NVT ensemble, since this corresponds to the way recent experiments were done,^{13,26} although our parameters do not strictly allow to reproduce these experiments. For each system studied, we performed a full heating and cooling cycle, where for each temperature, we used 1.0×10^6 MD steps for equilibration and 2.5×10^5 MD steps for sampling. There was no visible hysteresis in pressure or total energy during the cycles, which we take as a sign that our sampling is sufficient. Also, even in the crystalline phase, particles were on average moving about 7 particle diameters during each sampling phase, so that it is unlikely that the simulations sample only a local minimum. Errors were estimated *a posteriori* by a binning procedure. For our simulations the software package ESPResSo version 2.1.2j was used.⁴²

III. RESULTS AND DISCUSSION

To check whether the system is in a hexatic phase, one usually studies the decay of the radial distribution function $g(r)$ and the correlation of the local bond-order parameter, G_6 . Alternatively, one can check the orientational susceptibility χ_6 ,^{24,27} or the modified susceptibility χ'_6 ,^{13,25,43} and (to our knowledge used only in strictly 2D systems before) the Binder cumulant of ψ_6 .^{25,44}

We would like to introduce these parameters at the example of the system accommodating one layer and with the wall attraction $\epsilon_w = 5$. All parameters are based on the local bond-order correlation parameter since the hexatic phase is characterized by quasi-long-range bond order. The local bond-order

correlation parameter of particle j in layer m at a position \mathbf{x}_j is defined as

$$\psi_6(\mathbf{x}_j) = \frac{1}{N_j} \sum_{k=1}^{N_j} e^{i6\theta_{jk}}, \quad (3)$$

where N_j is the number of neighbors of particle j within layer m , the sum is over the neighbors k of j within m , and θ_{jk} is the angle between an arbitrary fixed axis and the line connecting particles j and k . The order parameter of the layer Ψ_6 is defined as the average over $\psi_6(\mathbf{x}_j)$ for all N particles within the layer,

$$\Psi_6 = \frac{1}{N} \left| \sum_{j=1}^N \psi_6(\mathbf{x}_j) \right|. \quad (4)$$

The correlation function $G_6(r)$ of the local bond-orientational order helps to distinguish long- and short-range orientational orders. It is defined as

$$G_6(r) = \langle \psi_6^*(\mathbf{x}') \psi_6(\mathbf{x}) \rangle, \quad (5)$$

where the average is taken over all particles within a layer where positions \mathbf{x}' and \mathbf{x} are a distance r apart. The radial distribution function in turn allows to distinguish long- and short-range translational orders and is defined as

$$g(r) = \langle \rho(r) \rangle / \rho, \quad (6)$$

where $\langle \rho(r) \rangle$ denotes the average local density at distance r from a fixed particle and ρ is the overall average density.

Ideally, the decay of G_6 together with the radial distribution function $g(r)$ (RDF) allows to detect a hexatic phase. For a two-dimensional crystal with long-range orientational and translational order, G_6 flattens to a nonzero constant, while $g(r)$ decays very slowly to 1. In a two-dimensional liquid, we have only short-range order, and therefore both functions decay exponentially to 0 and 1, respectively. In the hexatic phase with its long-range orientational, but short-range translational order, G_6 decays algebraically, while $g(r)$ decays exponentially.

As shown in Fig. 1, the radial distribution for $T = 5.05, 5.15$ is still quasi-long ranged and solidlike, and for $T = 5.2, 5.25$, and 5.35 the RDF looks like the one for liquid. Meanwhile, G_6 only for $T = 5.05$ does not show any decay, for $T = 5.15$ and 5.2 it decays algebraically and starting with $T = 5.25$ it decays exponentially. Combining conclusions from RDF and G_6 one can suspect that around $T = 5.2$ there is a hexatic phase and at $T = 5.15$ we have a defective crystal. However, the crossover to exponential decay at $T = 5.25$ happens at very long distances above 20 particle diameters. To reliably detect the type of decay, we would need $G_6(r)$ for distances of at least an order of magnitude more, that is above 200 in our case. Simulations in such a large box would be extremely time consuming, which would be unfeasible with our resources.

However, both G_6 and the RDF are averaged over the whole system, so if the system is not homogeneous, they cannot detect that. The obvious way to check the homogeneity, except for a direct observation, is to divide the original system into several subsystems and to compare the behavior of

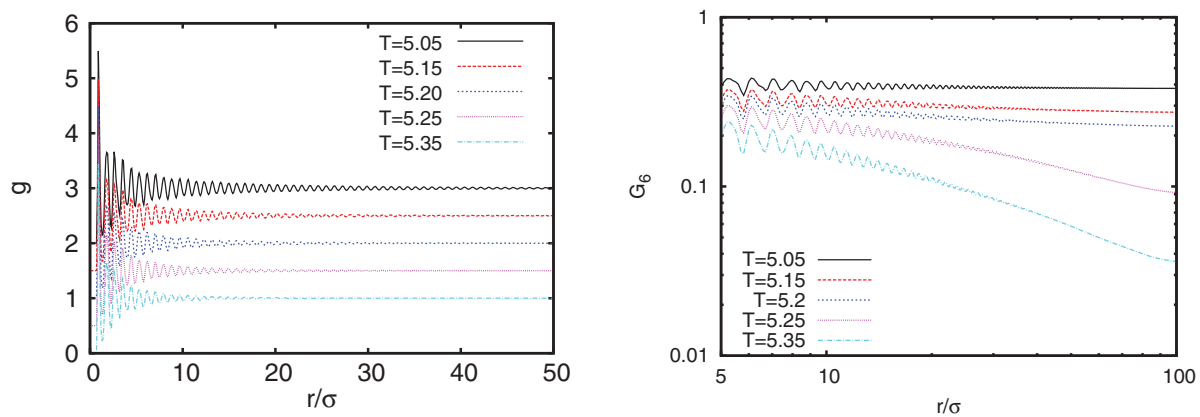


FIG. 1. Left figure: Radial distribution function $g(r)$ for one layer, $\epsilon_w = 5$ versus r/σ . The curves are shifted along the y axis to separate them, temperatures: 5.05, 5.15, 5.2, 5.25, 5.35 from top to bottom. The RDF for $T = 5.05, 5.15$ is quasi-long ranged and solidlike, and for $T = 5.2, 5.25$, and 5.35 it is short ranged as for liquid. Right figure: Correlation function $G_6(r)$ of the bond order parameter versus r/σ . Temperatures: 5.05, 5.15, 5.2, 5.25, 5.35 from top to bottom. G_6 does not decay for $T = 5.05$, for $T = 5.15$ and 5.2 it decays algebraically, for $T = 5.25$ and 5.35 G_6 decays exponentially.

the parameters in each of subbox. Calculating G_6 in subsystems is not favorable, since we are interested in the long-range decay that becomes impossible to study with decreasing system size.

In Ref. 24, a study of the nearest-neighbor bond-angular susceptibility on various length scales was performed. The susceptibility is defined as

$$\chi_6 = \left\langle \left| \frac{1}{N} \sum_j \psi_6(\mathbf{x}_j) \right|^2 \right\rangle = \langle \Psi_6^2 \rangle. \quad (7)$$

This quantity is used to examine the system on different length scales by dividing the system into equal subblocks of length $L_b = L/2, L/4, \dots, L/64, L/128$, where L is the box length of the original system. For each subblock the distribution of χ_6 was computed. In the solid χ_6 will be between 1 and 0.5 due to the presence of the long-range order and in the liquid χ_6 will be close to zero. In Fig. 2 (left), we show the distribution of χ_6 at $T = 5.2$, where the hexatic phase is suspected. One can see that the distribution has one peak, so the phase should be homogeneous at this temperature. The χ_6 peak gradually shifts away from 0.5 and becomes wider

with increasing temperature and then, at $T = 5.25$, the system changes into the liquid state (Fig. 2 (right)). Again, this supports the idea that at $T = 5.2$ the system goes through a hexatic phase.

If the system is inhomogeneous, a combination of solid and liquid distributions for subblocks with small length is observed, a vivid example is shown in Fig. 3 (right) for the two layers system at $T = 3.8$. In all two-layer systems for different wall attraction we could see only three regimes: solid, liquid, or a solid-liquid coexistence. As expected, the radial distribution function and the correlation of the bond-order parameter do not capture this (Fig. 3 (left)). The RDF of up to $T = 3.8$ is still quasi-long range and then at $T = 3.85$ it becomes short range. The decay of the G_6 at $T = 3.8$ is algebraic, at $T = 3.85$ it shows a combination of algebraic and exponential decays and at $T = 3.9$ it becomes purely exponential (see the inset Fig. 3 (left)). No homogeneous phase in the intermediate region was observed for any of the wall-particle attractions we studied.

Bagchi *et al.*²⁷ analyzed the scaling of the logarithm of the ratio $\chi_6(L_b)/\chi_6(L)$ versus $\ln(L_b/L)$. In the isotropic phase, the slope should be -2 and in the hexatic phase it will

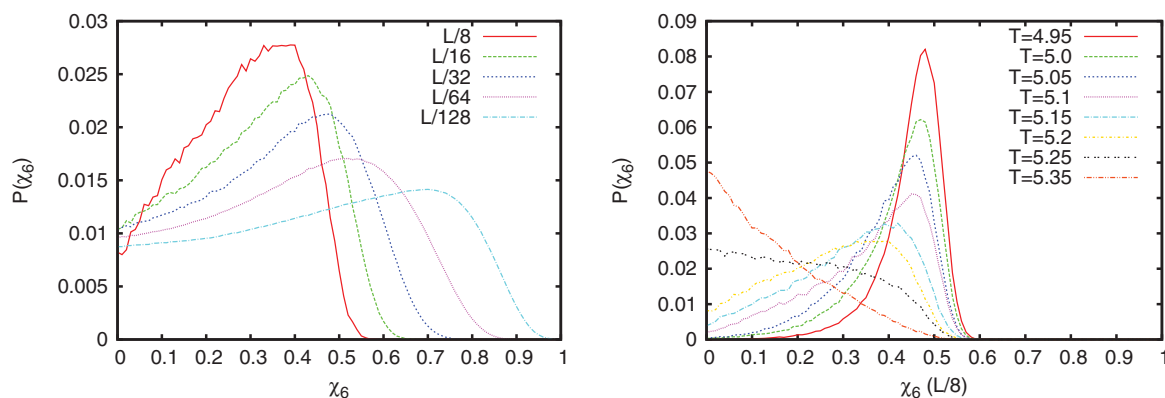


FIG. 2. Left figure: The distribution of χ_6 for $L/128, L/64, \dots, L/8$ subdivisions (from right to left) of the box at $T = 5.2$ in one layer, $\epsilon_w = 5$, where we suspected a hexatic phase. The distribution has one peak and the phase is homogeneous. Right figure: The distribution of χ_6 for subdivision $1/8$ at temperatures 4.95, 5.0, \dots , 5.25, 5.35 (from right to left). The peak of the distribution gradually shifts away from 0.5 and becomes wider with increasing temperature, then at $T = 5.25$ the system changes into the liquid state.

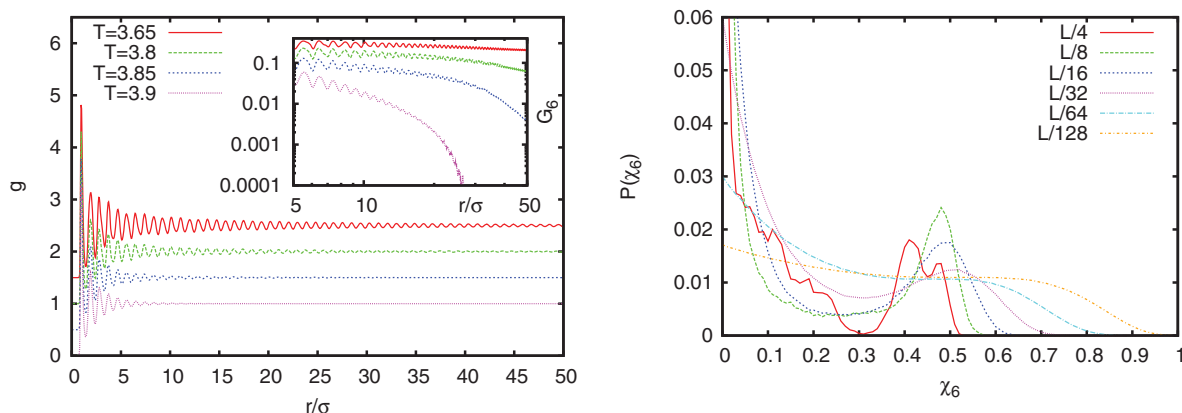


FIG. 3. Left figure: The radial distribution function for temperatures 3.65, 3.8, 3.85, and 3.9 (from top to bottom) in two layers. The RDF for $T = 3.65$ and $T = 3.8$ still behaves solidlike and for $T = 3.85$ and $T = 3.9$ it shows the liquidlike behavior. Inset: Correlation of the bond order parameter G_6 for the same temperatures as the RDF. G_6 decays algebraically up to $T = 3.8$, for $T = 3.85$ it has at first an algebraic decay and that becomes later exponential, at 3.9 G_6 decays exponentially. Right figure: The distribution of χ_6 for $L/128$, $L/64$, \dots $L/4$ subdivisions of the box (from right to left) at $T = 3.8$ in two layers, $\epsilon_w = 5$. The distribution has two peaks around 0.5 and 0 that shows that the system has a liquid-solid coexistence.

be $-\eta_6 \leq -1/4$. For the crystal without defects there should be no scaling. This relation is widely used to check the presence of the hexatic phase and finite size effects. In Fig. 4, we present the results of the scaling for our system. Due to defects in the crystal the scaling for low temperatures is not linear. The dotted line with the slope $-1/4$ reproduces the maximum slope expected in the hexatic phase. As we can see from Fig. 4, the slope of the scaling curve for $T = 5.25$ is very close to $1/4$, but we already know that the corresponding G_6 decays on long distances exponentially, so, most probably, at this temperature no hexatic phase exists. The scaling for lower temperatures does not allow us to distinguish between a crystal with many defects and a probable hexatic phase. The scaling for $T = 5.2$, where we expected the hexatic behavior, does not look any different from the one for $T = 5.15$, that we verified as a crystal. We conclude that while the distribution of χ_6 is a good parameter to detect a possible two-phase region, it is difficult to detect a hexatic phase by it alone, since the distribution of χ_6 in both liquid and crystal is rather broad, so

that the intermediate hexatic phase can be easily overlooked. The subblock scaling of χ_6 is more sensitive, but as we have shown, cannot distinguish a defective crystal from a hexatic phase.

Another version of susceptibility,^{25,43} $\chi'_6(L_b)$, measures the fluctuations of the bond-order parameter in the system,

$$k_B T \chi'_6 = L_b^2 (\langle \Psi_6^2(L_b) \rangle - \langle \Psi_6(L_b) \rangle^2). \quad (8)$$

It should show a dramatic increase as the transition temperatures are approached either from solid or from liquid phases and for the hexatic region it should become infinite.²⁵ However, it is impossible to produce infinity in the simulations, therefore, a large, but finite value is expected. χ'_6 is presented in Fig. 5 (left) as a function of temperature, both for our standard system with $L_y = L_z = 200$ and a smaller one with $L_y = L_z = 100$ to show that the size effects are very small. We compare χ'_6 for subdivisions $L/64$ and $L/128$ in the bigger system that correspond to $L/32$ and $L/64$ in the smaller system. The two comparable subdivisions of the two different realizations agree within error bars, which indicates that the system is sampled sufficiently well. We can see that the maxima of all curves are shifted to the liquid phase to $T = 5.35$, which is a consequence of the finite size effects in first order transitions.^{25,45} The dashed line marks the temperature $T = 5.2$, where some signs of the hexatic phase were observed, here we do not see any special features. The right part of Fig. 5 displays the dependence of χ'_6 on the inverse value of the length of a subbox. If we do not subdivide the box, the scaling breaks down as we can clearly see on the graphs (first points). This failure can be explained by the fact that we simulate in the canonical ensemble, but as soon as we start subdividing the system, it behaves more like a grand-canonical ensemble. Unfortunately, we cannot extrapolate our curves to χ_∞ as it was done in Ref. 25 since our way of subdivision does not provide enough data in the linear region of the curve. What we can still see is that the steepest slope is observed for temperature 5.35, and we already know that this temperature lies in the liquid state region. We can conclude that the observed transition is of a first order, but, as expected,

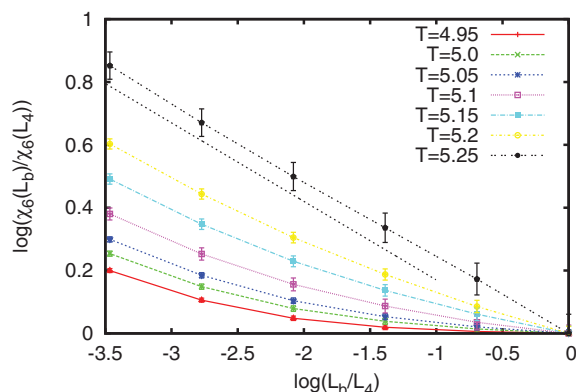


FIG. 4. Subblock scaling analysis for χ_6 , in one layer, $\epsilon_w = 5$ for temperatures 4.95, 5.0, \dots 5.25 (from bottom to top). The dotted line corresponds to a slope $-1/4$, the maximum possible slope for a hexatic phase. The slope of χ_6 at $T = 5.25$ is close to $-1/4$, for the other temperatures it is lower. If not visible, error bars are smaller than the symbols. The observed nonlinearity is due to defects.

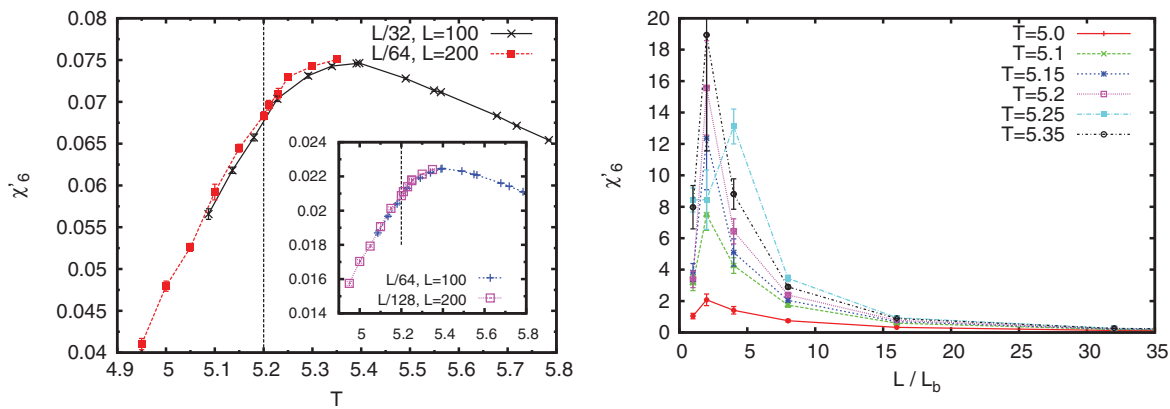


FIG. 5. Left figure: Fluctuation of the bond-order parameter, χ'_6 , as a function of temperature, in one layer, $\epsilon_w = 5$ for systems with box-lengths 100 and 200 for different subdivisions. The dashed line marks $T = 5.2$, where we suspected a hexatic phase. The maxima of the curves are shifted to the liquid region. Size effects are small. Inset shows χ'_6 for the next smaller subdivision, $L/64$ and $L/128$, respectively. If not visible, error bars are smaller than the symbols. Right figure: χ'_6 as a function of number of subboxes per side L/L_b , where L_b is the subbox length. The steepest slope is observed for temperature 5.35, which is in the liquid phase.

the transition temperatures obtained with this parameter are too high.

The last order parameter we investigate is the Binder cumulant,^{25,44}

$$U_L = 1 - \frac{\langle \Psi_6^4 \rangle}{3\langle \Psi_6^2 \rangle^2}. \quad (9)$$

Away from criticality in the limit of infinite system size, the cumulant assumes different limiting values for ordered and disordered phases. For finite systems, the value of the cumulant depends on the system size: the smaller the system, the more the cumulant deviates from the limiting value. In the case of a first order transition, the cumulant exhibits an effective common intersection point at the transition for sufficiently large systems. As for the hexatic phase, the cumulant is expected to be independent of the system size and to collapse onto one line over the entire range of the phase. Figure 6 (left) presents the behavior of the cumulant with temperature (lines serve as guides to the eye). We see clearly that there is only one intersection point, meaning that there is one first order solid-liquid transition and no hexatic phase.

Summarizing all our investigations we have shown that one should be quite careful in choosing the order parameters in order to claim to have observed a hexatic phase. In our case, the Binder cumulant provided the most stringent test.

What would happen if the attraction of the walls becomes even more attractive? Let us look at the case $\epsilon_w = 7$. We will start from the last parameter we considered previously, U_L given by Eq. (9), since we claimed that this was the most sensitive parameter. As one can see in Fig. 6 (right), there is a small interval for temperatures between 5.44 and 5.46 where the curves for different subdivisions of the system almost fall together. We interpret this as a sign of a possible hexatic phase, since here the cumulant is independent of the system size. However, the temperature interval is extremely narrow, so that the collapse of U_L might not show a new phase itself, but might be a precursor of a hexatic phase that would appear at higher wall attraction or might happen only for infinite wall attraction.

The distribution of χ_6 (Eq. (7)) in the possible hexatic phase, $T = 5.45$, shows that the system is homogeneous (Fig. 7, left). If we look at the behavior of the χ_6

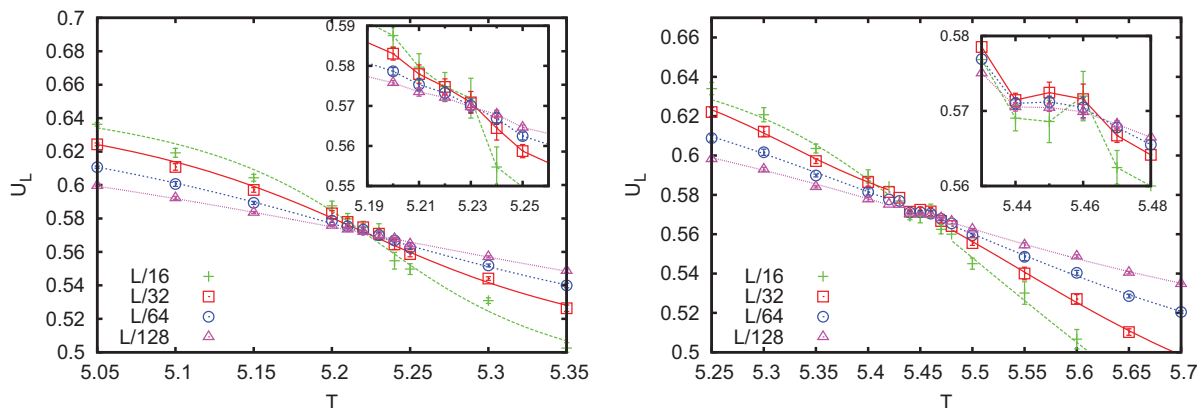


FIG. 6. Left figure: The Binder cumulant U_L for several subdivisions of the system in one layer, $\epsilon_w = 5$ as a function of temperature. The curves do not collapse anywhere and intersect around $T = 5.23$ (see inset), meaning that there is one first order solid-liquid transition and no hexatic phase. Lines are guides to the eye. If not visible, error bars are smaller than the symbols. Right figure: The Binder cumulant U_L for several subdivisions of the system in one layer, $\epsilon_w = 7$. The curves are almost collapsing on one curve between temperatures 5.44 and 5.46 (see inset), a sign of a possible hexatic phase. Lines are guides to the eye.

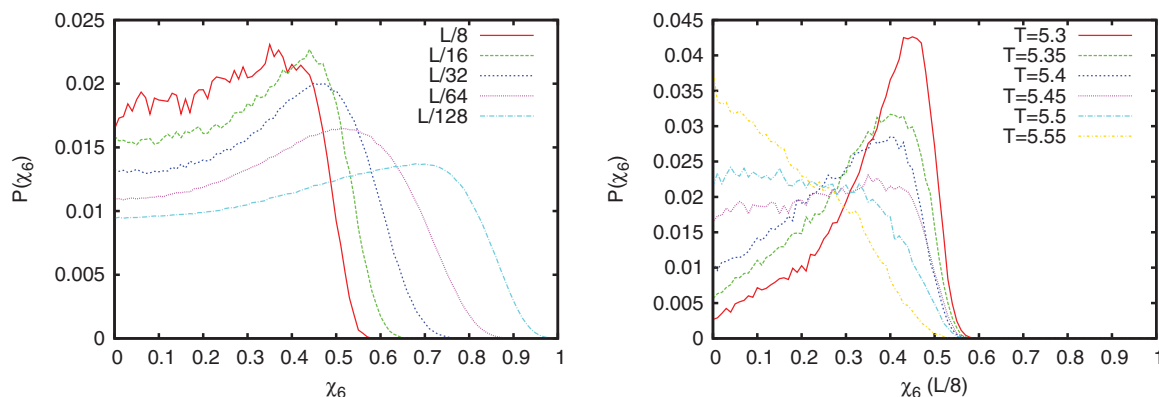


FIG. 7. Left figure: The distribution of χ_6 for $L/128, L/64, \dots, L/8$ subdivisions of the box (from right to left) in hexatic phase at $T = 5.45$ in one layer, $\epsilon_w = 7$. The distribution has one peak and the phase is homogeneous. Right figure: The distribution of χ_6 for subdivision $1/8$ at temperatures $5.3, 5.35, \dots, 5.55$ (from right to left). The peak of the distribution gradually shifts away from 0.5 and becomes wider with increasing temperature and then at $T = 5.55$ the system changes into the liquid state.

distribution (Fig. 7 right), taking as an example the subdivision into 8×8 subblocks, we observe again that the peak of the distribution decreases and slowly moves to lower values of χ_6 with increasing temperature. We do not see any peculiarities in the distribution for $T = 5.45$, and at $T = 5.55$ we observe a change to the characteristic liquid distribution with the maximum at 0 .

Also the behavior of other parameters, such as the radial distribution function and the correlation of the bond-order parameter or scaling of χ_6 , does not qualitatively differ from the behavior in the case of a less attractive wall $\epsilon_w = 5$, so we go through them briefly.

The correlation of the bond-order parameter decays algebraically for temperatures up to $T = 5.5$ (inset of Fig. 8), and at $T = 5.35$ and further on we see a short-range behavior of the radial distribution function (Fig. 8). However, we already know that for $T = 5.35$ and 5.4 there is no hexatic phase and we deal with a defective crystal. So, we conclude, that a combination of RDF and G_6 is unreliable for claiming

the occurrence of a hexatic phase, since it does not distinguish it from a defective crystal.

The scaling of the $\chi_6(L_b)/\chi_6(L_4)$ for temperatures up to $T = 5.45$ is below the $1/4$ slope (Fig. 9). For $T = 5.5$ the scaling of the ratio is exactly 0.25 . The distribution of χ_6 for 5.5 is also not yet liquid (Fig. 7). Therefore, according to distribution and scaling of χ_6 and G_6 at the temperature 5.5 the system has hexatic properties, but for the cumulant U_L it is already in the liquid phase. On the one hand, since we do not observe any two-phase region between a hexatic and liquid phase, one can assume that the Binder cumulant is oversensitive and can omit some points. On the other hand, the transition from the hexatic to the liquid state proceeds very smoothly and the temperature 5.5 can be treated as a boundary temperature between two phases.

If we look at the change of $\chi'_6(L)$ (Eq. (8)) with temperature, we observe maxima between the temperatures 5.6 and 5.65 (Fig. 10), which indicate that the transition to the liquid is of first order, since the maxima for this parameter are far in the liquid phase. However, no change in behavior is observed in the possible region of a hexatic phase, the borders of which are marked with dashed lines. We compare again the

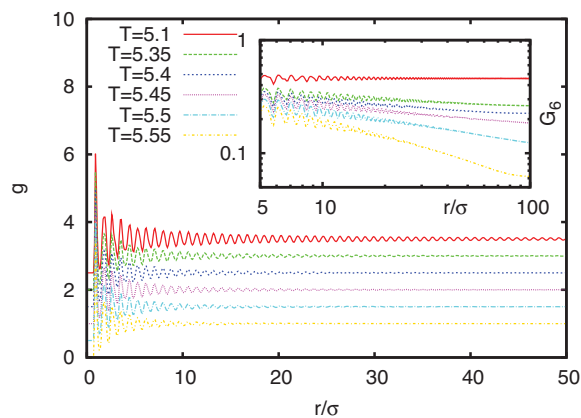


FIG. 8. Radial distribution function $g(r)$ for one layer, $\epsilon_w = 7$ for temperatures $5.1, 5.35, 5.4, \dots, 5.55$ (from top to bottom). The curves are shifted along the y axis to separate them. RDF for $T = 5.1$ is quasi-long ranged and solidlike, already at $T = 5.35$ it is short ranged as for liquid. Inset: Correlation of the bond-order parameter g_6 in one layer, $\epsilon_w = 7$ (same temperatures as for RDF). For $T = 5.1$ it does not decay; for $T = 5.35, 5.4, 5.45, 5.5$, it decays algebraically and for $T = 5.55$ G_6 decays exponentially.

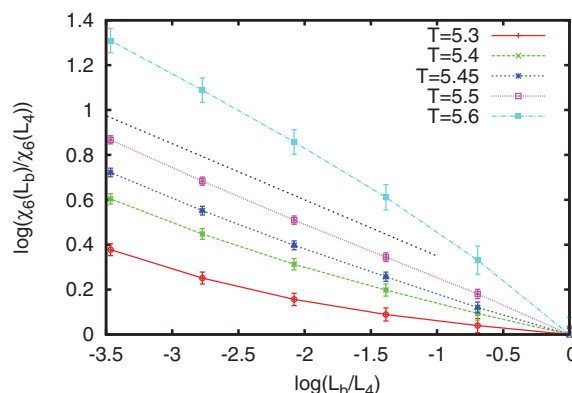


FIG. 9. Subblock scaling analysis for χ_6 , in one layer, $\epsilon_w = 7$ for temperatures $T = 5.3, 5.4, 5.45, 5.5, 5.6$ (from bottom to top). The dotted line corresponds to a slope $-1/4$, the maximum possible slope for a hexatic phase. If not visible, error bars are smaller than the symbols.

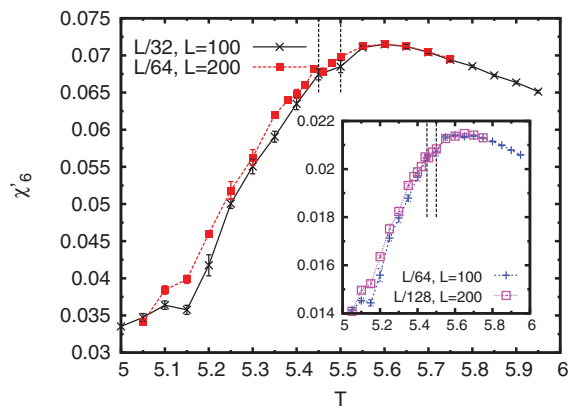


FIG. 10. Fluctuation of the bond-order parameter, χ'_6 , as a function of temperature, in one layer, $\epsilon_w = 7$, for systems with box-lengths 100 and 200 for $L/32$ and $L/64$ subdivisions correspondingly. Dashed lines mark the region of a hexatic phase. Maxima of curves are shifted to the liquid region. Size effects are small. Inset shows χ'_6 for the next smaller subdivision, $L/64$ and $L/128$, respectively. If not visible, error bars are smaller than the symbols.

behavior of $\chi'_6(L)$ for subdivisions $L/64$, $L/128$ in our standard system with box-length 200 and $L/32$, $L/64$ in a smaller one with $L_y = L_z = 100$. The curves for the corresponding subdivisions coincide within error bars in the solid without defects and the liquid region. They show a small quantitative difference when the crystal gains defects and then goes to the hexatic phase, which region is marked by two dashed lines.

We have shown that only the Binder cumulant behaves qualitatively different for the systems with $\epsilon_w = 5$ and $\epsilon_w = 7$. The behavior of the other parameters is similar for both cases. In our simulations, the Binder cumulant shows signs of a hexatic phase only at the strongest wall attraction $\epsilon_w = 7$. We checked the fluctuations of particles perpendicular to the walls by fitting the density profile to a Gaussian distribution. The standard deviation for $\epsilon_w = 5$ is $\Delta z \approx 0.175$ and $\Delta z \approx 0.15$ for $\epsilon_w = 7$, practically independent of the temperature in the studied range. Both values are significantly smaller than 0.4, which was reported to be the maximally possible fluctuations for liquid-to-hexatic transition in the quasi-2D system of hard spheres.³⁹ Since our Lennard-Jones particles are much softer than hard spheres and therefore can overlap to some extent, this might explain why we need a stricter confinement to observe a hexatic phase.

IV. CONCLUSIONS

We carried out a simulation study of the liquid-to-solid transformation of a LJ fluid in a slit pore accommodating one or two layers and several ratios of wall-particle to particle-particle attractions. To investigate the possible existence of an intermediate hexatic phase that was previously observed not only in 2D, but also in quasi-2D systems,^{10,29,39} we performed an analysis using a broad range of order parameters.

Studying the radial distribution function $g(r)$ together with the decay of the bond-order correlation $G_6(r)$ turned out to be insufficient to investigate the phase behavior, since, on the one hand, they characterize the system as a whole and do not allow to detect phase separation. On the other hand, the

(possible) crossover from algebraic decay to exponential decay happens only at large distances, which requires very large and computationally expensive simulation boxes.

The angular susceptibility χ_6 turned out to be a good tool to detect phase coexistence, but cannot distinguish properly between a defective crystal and a hexatic phase, and therefore also does not allow to investigate the phase behavior alone. The modified susceptibility χ'_6 is more sensitive, but again requires much larger simulation boxes.

We consider the Binder cumulant U_L to be the most reliable parameter in detecting a hexatic phase already for relatively small system sizes. However, one should study in addition also the distribution of the angular susceptibility χ_6 in order to exclude a possible phase coexistence.

We observed signs of a possible intermediate hexatic phase only in the slit with extremely attractive walls and a single layer of particles, i.e., if the system is practically 2D, otherwise there is a single liquid-solid transition. This is in contrast to the works^{29,36} on a similar system, in which signs of a hexatic phase in the contact layers near the wall were observed even in systems with up to seven layers, at wall strengths comparable to our $\epsilon_w = 7$. These findings, however, were based on studying the behavior of global order parameters and scaling of Ψ_6 only, which, as we have shown, are not sufficient to safely detect a hexatic phase.

In our work the temperature of the transition computed with the help of U_L does not coincide with the temperature where the fluctuation of the bond-order parameter has a maximum, which makes it possible to assume a first order transition in all cases we studied.²⁵

Our results have implications for experimental studies on the hexatic phase,^{11,14} since they show that even a monolayer requires a strong confining force to exhibit a true hexatic phase, while studies based on the decay of the RDF and G_6 can easily be fooled by defective crystals or coexistent phases. This might explain why some studies find a hexatic phase, while other studies of a seemingly very similar system do not.

ACKNOWLEDGMENTS

The authors thank K. Binder for valuable remarks. N.G. benefited from fruitful discussions with E. E. Tareyeva, V. N. Ryzhov, and M. Sega. We thank the DFG for financial support through the SPP 1296 and the SRC "SimTech".

- ¹C. Alba-Simionesco, B. Coasne, G. Dosseh, G. Dudziak, K. E. Gubbins, R. Radhakrishnan, and M. Sliwiska-Bartkowiak, *J. Phys.: Condens. Matter* **18**, R15 (2006).
- ²U. Gasser, *J. Phys.: Condens. Matter* **21**, 203101 (2009).
- ³U. Gasser, C. Eisenmann, G. Maret, and P. Keim, *ChemPhysChem* **11**, 963 (2010).
- ⁴L. D. Gelb, K. E. Gubbins, R. Radhakrishnan, and M. Sliwiska-Bartkowiak, *Rep. Prog. Phys.* **62**, 1573 (1999).
- ⁵M. Miyahara and K. E. Gubbins, *J. Chem. Phys.* **106**, 2865 (1997).
- ⁶V. N. Ryzhov and E. E. Tareyeva, *Phys. Rev. B* **51**, 8789 (1995).
- ⁷V. Ryzhov and E. Tareyeva, *Physica A* **314**, 396 (2002).
- ⁸C. H. Mak, *Phys. Rev. E* **73**, 065104 (2006).
- ⁹S. I. Lee and S. J. Lee, *Phys. Rev. E* **78**, 041504 (2008).
- ¹⁰K. Binder, S. Sengupta, and P. Nielaba, *J. Phys.: Condens. Matter* **14**, 2323 (2002).
- ¹¹C. A. Murray and D. H. Van Winkle, *Phys. Rev. Lett.* **58**, 1200 (1987).
- ¹²A. H. Marcus and S. A. Rice, *Phys. Rev. Lett.* **77**, 2577 (1996).

- ¹³Y. Han, N. Y. Ha, A. M. Alsayed, and A. G. Yodh, *Phys. Rev. E* **77**, 041406 (2008).
- ¹⁴K. Zahn, R. Lenke, and G. Maret, *Phys. Rev. Lett.* **82**, 2721 (1999).
- ¹⁵K. Zahn and G. Maret, *Phys. Rev. Lett.* **85**, 3656 (2000).
- ¹⁶P. Keim, G. Maret, and H. H. von Grünberg, *Phys. Rev. E* **75**, 031402 (2007).
- ¹⁷J. M. Kosterlitz and D. J. Thouless, *J. Phys. C* **6**, 1181 (1973).
- ¹⁸B. I. Halperin and D. R. Nelson, *Phys. Rev. Lett.* **41**, 121 (1978).
- ¹⁹D. R. Nelson and B. I. Halperin, *Phys. Rev. B* **19**, 2457 (1979).
- ²⁰A. P. Young, *Phys. Rev. B* **19**, 1855 (1979).
- ²¹K. J. Strandburg, *Rev. Mod. Phys.* **60**, 161 (1988).
- ²²S. Rice, *Chem. Phys. Lett.* **479**, 1 (2009).
- ²³K. Wierschem and E. Manousakis, *Phys. Rev. B* **83**, 214108 (2011).
- ²⁴K. J. Strandburg, J. A. Zollweg, and G. V. Chester, *Phys. Rev. B* **30**, 2755 (1984).
- ²⁵H. Weber, D. Marx, and K. Binder, *Phys. Rev. B* **51**, 14636 (1995).
- ²⁶Y. Peng, Z. Wang, A. M. Alsayed, A. G. Yodh, and Y. Han, *Phys. Rev. Lett.* **104**, 205703 (2010).
- ²⁷K. Bagchi, H. C. Andersen, and W. Swope, *Phys. Rev. Lett.* **76**, 255 (1996).
- ²⁸A. Jaster, *Phys. Lett. A* **330**, 120 (2004).
- ²⁹R. Radhakrishnan, K. E. Gubbins, and M. Sliwinska-Bartkowiak, *Phys. Rev. Lett.* **89**, 076101 (2002).
- ³⁰M. A. Bates and D. Frenkel, *Phys. Rev. E* **61**, 5223 (2000).
- ³¹S. Sengupta, P. Nielaba, and K. Binder, *Phys. Rev. E* **61**, 6294 (2000).
- ³²K. W. Wojciechowski, K. V. Tretiakov, A. C. Branka, and M. Kowalik, *J. Chem. Phys.* **119**, 939 (2003).
- ³³H. Bock, K. Gubbins, and K. Ayappa, *J. Chem. Phys.* **122**, 094709 (2005).
- ³⁴K. Ayappa and R. Mishra, *J. Phys. Chem. B* **111**, 14299 (2007).
- ³⁵M. Kahn, J.-J. Weis, C. Likos, and G. Kahl, *Soft Matter* **5**, 2852 (2009).
- ³⁶R. Radhakrishnan, K. E. Gubbins, and M. Sliwinska-Bartkowiak, *J. Chem. Phys.* **116**, 1147 (2002).
- ³⁷A. Vishnyakov and A. V. Neimark, *J. Chem. Phys.* **118**, 7585 (2003).
- ³⁸A. J. Page and R. P. Sear, *Phys. Rev. E* **80**, 031605 (2009).
- ³⁹X. Xu and S. A. Rice, *Phys. Rev. E* **78**, 011602 (2008).
- ⁴⁰A. H. Marcus and S. A. Rice, *Phys. Rev. E* **55**, 637 (1997).
- ⁴¹P. Karnchanaphanurach, B. Lin, and S. A. Rice, *Phys. Rev. E* **61**, 4036 (2000).
- ⁴²H. J. Limbach, A. Arnold, B. A. Mann, and C. Holm, *Comput. Phys. Commun.* **174**, 704 (2006); see <http://espressomd.org/>.
- ⁴³J. Lee and K. J. Strandburg, *Phys. Rev. B* **46**, 11190 (1992).
- ⁴⁴K. Binder, *Z. Phys. B* **43**, 119 (1981).
- ⁴⁵W. Strepp, S. Sengupta, and P. Nielaba, *Phys. Rev. E* **63**, 046106 (2001).